Available online at www.sciencedirect.com
SCIENCE DIRECT
C. R. Physique 6 (2005) 47–59
COMPTES RENDUS PHYSIQUE
http://france.elsevier.com/direct/COMREN/

Self-organization on surfaces/Auto-organisation sur les surfaces

X-ray methods for strain and composition analysis in self-organized semiconductor nanostructures

Till Hartmut Metzger [a,*], Tobias Urs Schülli [a,b], Martin Schmidbauer [c]

[a] *ESRF, BP 220, 6, rue Jules Horowitz, 38043 Grenoble cedex, France*
[b] *CEA DRFMC/SP2M, 17, rue des Martyrs, 38054 Grenoble cedex 9, France*
[c] *Humboldt Universität zu Berlin, Institut für Physik, Newtonstr. 15, 12489 Berlin, Germany*

Available online 12 January 2005

Presented by Guy Laval

Abstract

The fabrication of low-dimensional nanostructures (e.g. quantum wires or quantum dots) is presently among the most exciting challenges in semiconductor technology. The electronic and optical properties of these systems depend decisively on structural parameters, such as size, shape, elastic strain, chemical composition and positional correlation among the nanostructures. X-ray scattering methods have proven to be an excellent tool to get access to these parameters. Beyond its sensitivity to deformations of the crystal lattice, it is sensitive to fluctuations of the surface and interface morphology on length scales ranging from 0.1 nm up to several μm. The small dimensions and the corresponding weak scattering signal require the use of highly brilliant synchrotron radiation. Recent methodological developments and their application to the material system Ge on Si are discussed. ***To cite this article: T.H. Metzger et al., C. R. Physique 6 (2005).***

Résumé

Méthodes de rayons X pour l'analyse des déformations et des compositions des nano-structures semi-conductrices auto-organisées. La fabrication de nanostructures de basse dimension (par exemple, fils et boîtes quantiques) est actuellement un des défis les plus passionnants de la technologie des semi-conducteurs. Les propriétés optiques et électroniques de ces systèmes dépendent de façon décisive de paramètres structuraux tels que la taille, la forme, les contraintes élastiques, la composition chimique et les corrélations de position entre les nanostructures. Les méthodes de diffusion des rayons X se sont révélées parfaitement adaptées à l'obtention de ces paramètres. En plus de leur sensibilité aux déformations du réseau cristallin, elles renseignent sur les fluctuations de la morphologie des surfaces et interfaces à une échelle spatiale allant de 0.1 nm jusqu'à plusieurs micromètres. Les petites dimensions et le faible signal de diffusion correspondant nécessitent l'utilisation de rayonnement synchrotron extrêmement brillant. Les développements méthodologiques récents et leur application au système Ge sur Si sont discutés. ***Pour citer cet article : T.H. Metzger et al., C. R. Physique 6 (2005).***

Keywords: Nanostructures; Self-organization; X-ray scattering; Semiconductors; Synchrotron radiation; Anomalous scattering; Finite element

Mots-clés : Nanostructures ; Auto-organisation ; Diffusion des rayons X ; Semi-conducteurs ; Rayonnement synchrotron ; Diffusion anomale ; Éléments finis

* Corresponding author.
E-mail address: metzger@esrf.fr (T.H. Metzger).

1631-0705/$ – see front matter
doi:10.1016/j.crhy.2004.11.002

1. Introduction

1.1. Semiconductor nano-structures

Since the beginning of the past decade, advanced techniques of crystal growth have been explored to tailor the electronic properties of materials. This opens fascinating prospects of fabricating new materials with modified physical properties. The principle behind is based on the competition between the dimension of the structure and the de Broglie wavelength of the charge carriers. When the charge carriers are confined to values smaller than the de Broglie wavelengths – which amounts typically to a few tens of nanometers – the electronic band structure is substantially altered and depends on the extension of the spatial confinement. The effects due to localization are especially strong when the charge carriers are confined not only in one dimension, as in quantum wells, but in two (quantum wires) or even in all three dimensions (quantum dots). In the latter case, localized discrete states are induced and an atom-like luminescence spectrum is observed [1]. The optical properties of semiconductor quantum dots can be exploited to fabricate photonic devices, for example lasers with quantum dot active layers which exhibit increased temperature stability, high efficiency, and low threshold current [2,3]. Quantum dots could also lead to novel device applications in opto-electronics, data storage or quantum cryptography. For a comprehensive review see [4,5].

1.2. Self-organized fabrication

Technological applications require dense arrays of monodisperse nanoscale structures of identical shape. Initially, the most widely followed approach to forming quantum dots was through electron beam lithography of suitably small featured patterns. However, besides the fact that the spatial resolution of typically 30 nm is often not small enough, there is still a problem with the large amount of damage introduced during the fabrication process itself. Therefore, self-organized growth mechanisms [6] have attracted much interest. Under the conditions of the Stranski–Krastanow growth mode [7] first a couple of monolayers (wetting layer) grow layer by layer. This is followed by three dimensional growth of coherent, defect-free islands [8–10]. It is generally accepted that the equilibrium shape of such self-organized islands (often referred to as self-assembled islands) is determined by the balance of surface free energy and elastic strain energy. A large variety of shapes has been reported (experimentally and theoretically) in the literature [11–16]. However, it turns out that the evolution of the islands is also strongly influenced by kinetic limitations during growth, i.e. the final result depends strongly on the growth conditions. Also other factors, e.g. surface orientation, magnitude and sign of strain contribute to the complexity of growth. These further complications of growth are the main reasons why self-organized growth is still not completely understood. Structural characterization is one promising path to a better understanding and control of these processes.

1.3. X-ray diffuse scattering

The aim of the present article is to highlight the capabilities of recent X-ray diffuse scattering techniques for the nondestructive characterization of nanostructures. The main advantage of X-ray techniques is based on the high resolution in reciprocal space, which is a direct consequence of the high angular resolution of just a few seconds of arc. Therefore, X-rays are sensitive to very small changes of lattice parameters. Moreover, thanks to the coherence lengths of typically a few micrometers, information on electron density fluctuations on a larger length scale than atomic spacings can be obtained. In principle, the entire mesoscopic range can be covered by X-ray scattering.

X-rays interact only weakly with matter. Due to the small volume fraction of the mesoscopic structures compared with the X-ray penetration depth, the scattering signal is very small and has to be enhanced relative to the large signal from the underlying substrate. Therefore, interface- and surface-sensitive techniques using a grazing-incidence geometry and applying highly brilliant synchrotron radiation are among the most promising approaches. Combined with anomalous scattering at energies close to an absorption edge of one of the constituent elements adds chemical sensitivity to the techniques.

Since the spot sizes of X-ray beams are typically in the range of a few square millimeters, X-rays average statistically over large ensembles of nanoscale structures. Hence the data are very reliable concerning statistics. However, structural data can be evaluated from experimental results only if a single type of nanostructures predominates. Coexistence of different types of nanostructures – for example quantum dots with different shapes or sizes – seriously complicates a detailed analysis. Since the scattering signal of a single kind of structure is usually widely spread in reciprocal space, the coexistence of different sorts of structures leads to troublesome overlapping of the scattering features. In this sense X-ray techniques are complementary to imaging techniques such as high-resolution transmission electron microscopy [17] and scanning probe microscopy [18]. These latter methods probe the structure locally with high spatial resolution but with a restricted field of view and, thus, often with insufficient statistical significance. Also, analytical electron microscopy techniques [19] such as energy-filtered transmission electron microscopy [20], electron energy loss spectroscopy (EELS) [21,22] and energy-dispersive X-ray spectroscopy [23] are very useful.

As long as only small scattering volumes are involved, X-ray diffraction can simply be described by kinematical diffraction theory. The X-ray scattered amplitude is proportional to the Fourier transform of the dielectric polarizability. The periodic part of the polarizability gives rise to sharp Bragg peaks, whereas all non-periodic deviations from the ideal crystal structure lead to diffuse scattering in the vicinity of the Bragg peaks. However, when scattering geometries with grazing incidence conditions are utilized, the kinematical theory is no longer valid and needs some modifications. These modifications can be made in the framework of the distorted-wave Born approximation (DWBA) [24].

Independent of the actual scattering theory, the diffuse intensity contains information on the size, shape, positional correlation, local chemical composition and strain field of the nanostructures. Such a mixture is not easy to analyze in detail. It is therefore necessary to combine different X-ray scattering techniques of varying sensitivity to these structural properties. Moreover, owing to the loss of phase information in reciprocal space, the scattered intensities can usually not be directly translated to complete information in real space. A promising approach – called iso-strain scattering – has been developed by Kegel et al. [25,26]. Here structural information such as size, strain and compostion can be – under certain assumptions – evaluated directly from the X-ray diffuse intensity. Another possible way is to construct a specific structural model in real space. Then the finite-element method is utilized to calculate the strain field inside the structure. The result is then used as an input for subsequent X-ray scattering simulations. After comparison with the experiment, the structural model – which may include, for example, the shape, size, or composition – can be further refined until satisfactory agreement is achieved [27].

1.4. Outline of the article

Along with the fast developments in growth techniques, the corresponding field of X-ray diffuse scattering has been developed – both experimentally and theoretically – on a short timescale and excellent research has been undertaken (e.g. [4,24–38]). Several review articles can be found in literature describing the current state of the art in the application of X-ray scattering techniques to study the structure of self-organized hetero nano-structures [39–42] in which numerous important material systems are discussed.

Since, in recent years, the technique of anomalous diffraction has been developed and employed to add chemical sensitivity to the X-ray methods described in the review articles above, we will focus on the combination of grazing incidence techniques, i.e. grazing incidence diffraction (GID) and its combination with anomalous dispersion effects. The corresponding iso-strain-scattering (ISS) is compared to the technique of reciprocal space mapping and simulations based on the finite element method (FEM). As a typical example, the application of these methods is demonstrated for the system Ge on Si(001) by presenting an overview on recent results. The analysis of lateral and vertical dot correlations is beyond the scope of this review.

2. Techniques and data evaluation

2.1. Reciprocal space mapping and finite element simulations

A popular X-ray method giving access to strain and interdiffusion of self-organized islands is X-ray reciprocal space mapping (RSM). The method is based on the knowledge of the elastic properties as well as the lattice parameters of Si, Ge and SiGe alloys, in the present case. In the case of ⟨001⟩ as the growth direction, one considers the Poisson-ratio ν_{100} to calculate the response of a crystal that is deformed from its native lattice constant, a, to a value $a_{\parallel}$ in the plane. The corresponding change of the lattice parameter in growth direction $a_{\perp}$ is then calculated by

$$a_{\perp} = a \cdot \left(1 + \frac{1+\nu_{100}}{1-\nu_{100}} \cdot \frac{a-a_{\parallel}}{a}\right). \tag{1}$$

Measuring $a_{\parallel}$ and $a_{\perp}$ and using the known ν_{100} the equilibrium lattice parameter a can be derived from Eq. (1). Together with an appropriate lattice-parameter interpolation for the corresponding alloy [43] this yields the composition. However, in the Stranski–Krastanow growth mode of islands, one obtains neither perfect pseudomorphic growth with the in-plane lattice constant equal to that of Si, nor does one find a completely relaxed cubic unit cell of the deposited material. The dot material is usually in a state of partial elastic relaxation, which progresses with the height inside the islands. In reciprocal space one generally maps out the vicinity of a Bragg reflection, where the information about strain and composition can be found.

A quantitative evaluation of strain and composition can only be obtained from simulations calculating the diffuse scattering intensity distribution on the base of lattice displacements determined by finite element methods (FEM) [27].

The scattered amplitude $A(\boldsymbol{q})$ can be expressed in kinematical approximation as

$$A(\vec{q}) = \sum_k F_{\mathrm{h}}^{\mathrm{ideal}}(\vec{r}_k)\, \mathrm{e}^{\mathrm{i}\vec{q}\cdot(\vec{r}_k+\vec{u}_k)}. \tag{2}$$

The summation is performed over all unit cells k. In the undisturbed lattice they are located at positions $\boldsymbol{r}_k$, and $\boldsymbol{u}_k$ are their displacements in the disturbed lattice. $F_{\mathrm{h}}^{\mathrm{ideal}}$ is the structure amplitude of the undisturbed lattice. The components of the displacement field $\boldsymbol{u}(\boldsymbol{r}) = (u_1, u_2, u_3)$ that is used in the X-ray simulations are related to the (symmetrical) elastic strain tensor components ε_{ij}. On the basis of Eq. (2) various mechanisms of intensity contrast are possible:

(i) The scattering power depends on the atomic species inside the mesoscopic structure. Therefore, a change or gradient in the atomic composition may lead to a considerable fluctuation of the structure amplitude $F_{\mathrm{h}}^{\mathrm{ideal}}(\boldsymbol{r}_k)$. These fluctuations which are generally related to the growth process (e.g. interdiffusion or segregation) generate so-called structure factor contrast. Usually, the structure factor contrast is very weak for strongly strained systems but can be substantially amplified by performing anomalous scattering close to the absorption edge of one selected atomic species.
(ii) Intensity contrast can be also induced by strain inside the mesoscopic structure. The strain enters into the diffuse intensity via the phase $\boldsymbol{q} \cdot (\boldsymbol{r}_k + \boldsymbol{u}_k)$ and is generally inhomogenous, i.e., it depends on the location inside the mesoscopic structure.
(iii) The summation in Eq. (2) is performed over the entire mesoscopic structure, e.g. a nanoscale island with a limited size and a distinct shape. Therefore, truncation effects are visible in the intensity distribution. Among these effects are crystal truncation rods (CTR) and size fringes. These shape- and size-related features in diffuse scattering determine the form function in reciprocal space.

Usually, it is not straightforward to distinguish among these three effects. Moreover, strain, shape, size, and chemical composition cannot be directly extracted from the intensity distribution in reciprocal space. The diffuse-scattering intensity pattern has to be calculated by model assumptions that have to be refined until satisfactory agreement between simulation and experiment is achieved.

In the simulation of scattering data, one has to face problems concerning the direct access to the required information. Among them are the loss of phase information in intensity measurement, the superimposition of effects of strain, shape, and positional correlation, and the tensor character of strain. It has been tried to overcome the latter point by using analytical expressions to approximate the strain field, ensuring rapid calculations of strain. These analytical approaches have been applied for planar layers with steps [44], quantum wires [45], hut clusters [30], and rotationally symmetric islands [46]. They are, however, often empirical [30,45] and, owing to the complicated strain tensor field $\varepsilon_{ij}(x, y, z)$ not justified for complicated three-dimensional structures.

In recent years, the use of FEM to calculate the strain field in mesoscopic structures has been successfully established (e.g. [27,47,48]). The FEM is based on linear continuum elasticity theory, it includes the full elastic anisotropy, and it has proven to be applicable down to structure sizes of a few tens of nanometers. For object sizes below about 10 nm and at very high lattice mismatch (e.g. 7% for InAs quantum dots on GaAs), there are distinct deviations from elasticity theory and the atomic structure of the quantum dots has to be considered [49]. However, these atomistic calculations are mostly performed in the framework of the valence force field (VFF) method. Even with high-performance computers, true first-principles (ab initio) calculations are feasible only for systems containing fewer than about 100 atoms [50].

For the systems under consideration here, linear elasticity theory is valid. Wiebach et al. [27] have developed a 'brute force' iterative approach for data evaluation of nanoscale islands, which in general, cannot be used as a true 'fitting' procedure since there are too many free parameters in the model (shape, size, chemical composition, and spatial correlation). Therefore, it is advantageous to include knowledge obtained by other methods, e.g. information on the shape and size obtained by AFM, SEM, and TEM. An example of this technique will be given in the next section.

2.2. Scattering at grazing incidence and exit: GISAXS and GID

A typical task in the evaluation of structural parameters of quantum dots from the diffuse scattering is the discrimination of the dot-induced scattering from the strong signal of the substrate. A single layer of islands has a typical height of about 10 nm, which has to be compared with the penetration depth of the X-rays into the substrate ranging up to 100 μm. Thus the diffuse scattering from the islands needs to be enhanced as compared to the substrate contribution. The problem can be solved by combining refraction and diffraction, i.e. choosing the geometry of grazing incidence and exit. Since the index of refraction for X-rays in condensed matter is slightly smaller than unity, a critical angle for total external reflection α_{c} exists, in the neighborhood of which the penetration depth can be tuned between about 5 nm and 500 nm depending on the X-ray energy and the material used. Keeping the incident angle smaller than the critical angle α_{c}, typically 0.1 to 0.5 degree, the signal from the islands is enhanced by the transmission function up to a factor of 4 while the diffuse signal from the substrate is reduced considerably by the reduced penetration depth of the X-rays. The scattering geometry for grazing incidence diffraction (GID) and small angle X-ray scattering (GISAXS) is shown in Fig. 1. A well collimated incident X-ray beam impinges on the sample surface under a small angle α_{i} close to α_{c}. The scattered beam is collected in a fan of exit angles along α_{f} of about 2 degrees and is typically recorded by a linear position sensitive detector, PSD. In this non-coplanar, 3D scattering geometry the main

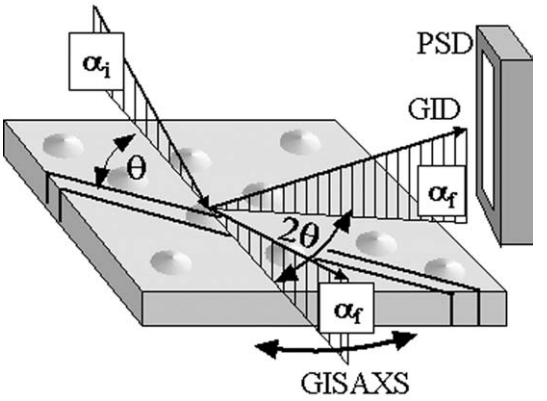

Fig. 1. Scattering geometry at grazing incidence and exit. The lateral momentum transfer is set by the angles θ and 2θ. The intensity along q_z is recorded by a linear position-sensitive detector (PSD).

component of the scattering vector is parallel to the sample surface. For GISAXS the scattering angle 2θ in the surface plane is small. As a consequence GISAXS is not sensitive to atomic distances but is a measure for length scales in the mesoscopic range well suited for nanometer-sized islands. With GISAXS the morphology (shape, size) and positional correlation of the islands can be quantified with high statistical accuracy since the X-rays average over macroscopic sample dimensions. The results obtained are complementary to those from real space techniques such as AFM or STM, in fact the latter are often used to take the shape and size of a single island as an input to model the scattering distribution of a GISAXS measurement. Since excellent review articles have been reported on this technique [37,42] we will not deal further with it here, but rather concentrate on GID.

For GID the lateral momentum transfer is large enough to reach nonzero Bragg points in reciprocal space from netplanes perpendicular to the surface. Since α_i and α_f are kept small to enhance the diffraction from the near surface regions of the sample, the Q_z component is close to zero. Therefore GID is sensitive to the in-plane strain only. Nevertheless, the Q_z dependence of the scattered intensity – as measured by a PSD – can be employed to analyze the vertical stacking of nano-structures buried in a multilayer [51] or to exploit multiple scattering channels to determine the height of certain strain states within freestanding islands (see Iso-Strain-Scattering technique in the next chapter).

2.3. Iso Strain Scattering (ISS): discrimination of strain and size

In general, the diffuse scattering intensity from uncapped nano-structures contains information on their shape, size, positional correlation, strain and chemical composition. For low area coverage, i.e. the distance between the islands is much larger than their base width, the island positions usually show a random distribution. In this case the diffuse scattering intensity is attributed to an average island. This is often a good approximation since their size and shape variation lies typically below 10%. For uncapped islands with sufficiently large lattice mismatch to the substrate, the ISS technique can be applied as first introduced by Kegel et al. [25,26]. Here, the scattering signal from the whole island is decomposed into scattering from iso strain areas as described in Fig. 2. In real space (Fig. 2(a)) the island must have a lattice parameter distribution varying monotonically with the height in the island, i.e. each iso-lattice parameter slice through the island can be attributed to a certain height and lateral width as indicated by the horizontal straight line through the island. The corresponding scattering signal from an individual slice is found in reciprocal space (Fig. 2(b)) as diffuse intensity with a maximum centered at $Q_r \propto 2\pi/a_{slice}$ in radial direction and extends in angular direction Q_a (perpendicular to Q_r) with a width inversely proportional to the lateral diameter of the slice. Consequently, large diameters at the bottom of the island and a lattice parameter close to the substrate will give a narrow intensity profile, while small slices at the relaxed top will result in a broad intensity distribution further away from the substrate peak. The corresponding relations are color coded in Fig. 2. If the lattice mismatch is large enough (or the measurements are performed at a high order reflection) the choice of Q_r allows one to probe a selected slice with the corresponding lattice parameter to which the scattering intensity distribution can be uniquely attributed. Along the angular direction Q_a the intensity distribution can then be modeled by the form-factor induced scattering of the slice and the diameter is determined directly from the measured intensity. In the case of high island symmetry the form-factor can often be expressed analytically.

In reality, the lattice parameter distribution and thus the intensity distribution is continuous and the results from the individual slices have to be interpolated to obtain the distribution of the lattice parameter as a function of the lateral size of the dot. The ISS technique can also be used to determine the height of an iso-strain area above the substrate by exploiting the Q_z dependences of the intensity from an individual slice. Due to multiple scattering processes described in [26], the intensity along α_f exhibits a

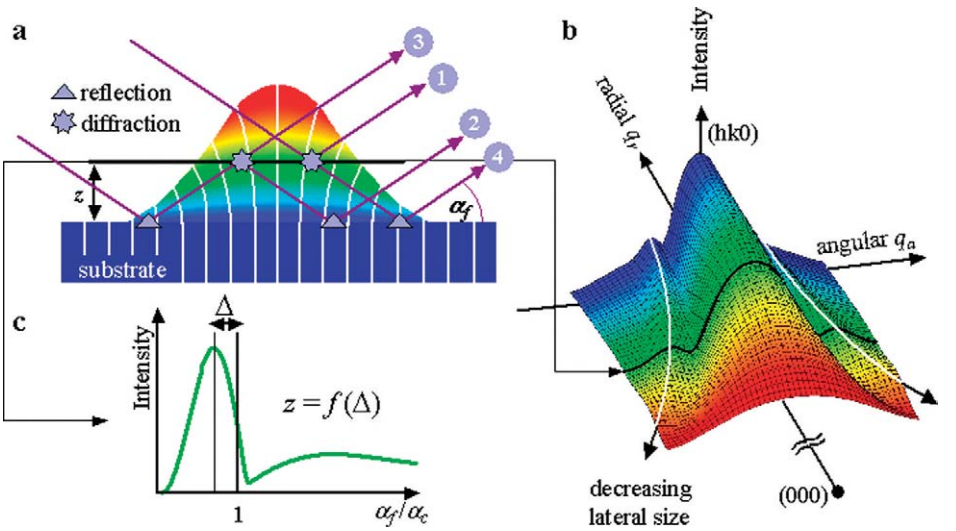

Fig. 2. Schematic representation of the model used for the data analysis by iso strain scattering. (a) Real space image of the coherent island with a lattice parameter increasing from the bottom to the top of the island. (b) Distribution of diffuse intensity close to the substrate peak (hk0). The lateral size of the slice through the island in a height z in (a) is obtained from the width of the corresponding intensity profile in angular direction q_a. (c) Intensity as a function of the exit angle with a shift of the maximum characteristic for the height z of the selected slice in (a). The shift Δ can be calculated using the four scattering channels indicated in (a).

shift of the Yoneda maximum which is characteristic for the height of an iso strain area above the sample surface. This extended DWBA is based on the four scattering channels as indicated schematically in Fig. 2(a), (c). The measurement at different Q_r yields the lattice parameter as a function of height. Combining the lateral and vertical information, i.e. on size, strain and height, a 3D image of the island can be reconstructed directly from the measured intensity distribution in reciprocal space. It is, however, restricted to the analysis of freestanding islands on a substrate. For buried islands grazing incidence is of limited value and the technique of reciprocal space mapping (RSM) combined with iterative model calculations using FEM is the more appropriate tool. This topic will be discussed in Section 3.2.

Since the strain distribution in an island is determined by relaxation and composition, and both influence the diffuse scattering distribution, it is necessary to separate the two effects. It is well known that intermixing of substrate and island material takes place during the growth at high temperature. The chemical composition within the islands can be determined by combining ISS with the anomalous dispersion of the atomic form factor of an element.

As shown in the following sections for the model system Ge on Si (4.2% lattice mismatch), this allows the determination of the vertical concentration profile by measuring the intensity along Q_r at two energies close to the Ge K-edge, while the lateral variation of the Ge concentration in the islands is obtained from measurements along Q_a. It is important to point out that at anomalous diffraction conditions the only quantity that is changed is the scattering power of Ge while all the other experimental details remain unchanged. Hence, the chemical composition can be deduced from the intensity ratio measured at two slightly different energies. Details are described in the following.

2.4. Anomalous scattering

While the surface sensitivity can be considerably enhanced with the grazing incidence method, one can further discriminate the scattering contributions of substrate and surface structures using anomalous scattering techniques. This exploits the change of the atomic scattering factor of an element, when the X-ray energy is chosen in the vicinity of an absorption edge. In the X-ray regime the K- or L-edges of the elements are of high relevance. The simplest approach consists of two diffuse scattering curves measured at two different energies in the vicinity of an absorption edge. The scattering contribution of the chosen element can then directly be attributed to each measured point in the probed region. The starting point for any experiment using the energy dependence of the atomic scattering factors is the quantitative knowledge of these factors for all involved elements. In general, the values given in the international tables are sufficient if one works far from resonance. The energy and momentum transfer dependency of the atomic scattering form factor is expressed by $f(Q, E) = f_0(Q) + f'(E) + \mathrm{i}f''(E)$.

$f'(E)$ and $f''(E)$ are the real and imaginary parts of the energy dependent corrections that become important close to an absorption edge. The real part of $f(Q, E)$ is relevant for scattering, whereas the imaginary part is describing the absorption of X-rays. The form factor f_0 represents the Fourier transform of the atomic electron density. Its Q dependence reflects the

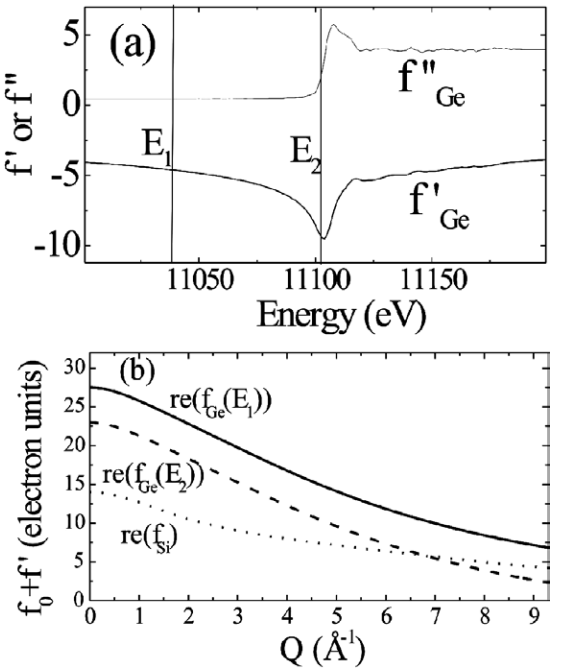

Fig. 3. Resonant correction terms f'_{Ge} and f''_{Ge} in the vicinity of the K-absorption edge. (b): real part of the complex atomic scattering factors for Ge (full and dashed line) at the energies marked in (a), and real part of f_{Si} (dotted line).

spatial distribution of the electrons in the atom. In the forward direction ($Q = 0$), f_0 equals the total number of electrons Z and decreases for higher momentum transfer Q. The momentum dependent decrease is generally neglected in the correction terms f' and f'', since the inner shell electrons, that are responsible for these terms, are strongly localized in space. Thus, the anomalous scattering effects can be enhanced considerably by measuring Bragg reflections for high momentum transfers and hence improve the sensitivity for the composition.

For the SiGe system, f' and f'' are presented in Fig. 3(a) as a function of energy. The two probed energies $E_1 = 11043$ eV and $E_2 = 11103$ eV are located at 61 eV and 1 eV below the Ge K-edge at 11104 eV. For a precise determination of the atomic scattering factors, one measures in general f'' via fluorescence or absorption. f' is then calculated using the Kramers–Kronig dispersion relation for the measured f'' values in the vicinity of the edge and values from the international tables for the remaining part of the spectrum. Fig. 3(b) shows that the anomalous effect can be enhanced from 20% at $Q = 0$ to about 80% at high Q.

3. 3D strain field and chemical composition in free-standing SiGe islands

3.1. Combination of ISS and anomalous diffraction

The surface sensitive diffraction methods introduced above have been combined and successfully applied to a variety of uncapped islands grown by molecular beam epitaxy (MBE) or chemical vapor deposition [42,52–55]. Particular effort has been spent to resolve the spatial composition gradient in SiGe-islands on Si(001). In order to achieve this goal, Schülli et al. [53] have applied anomalous diffraction to SiGe islands grown by MBE deposition of pure Ge on Si(001). From the radial scan at a high order reflection (800) at two relevant X-ray energies (Fig. 4) it becomes evident that up to a certain relaxation (indicated by the straight line in the figure), the dot consists of pure Si with a lattice parameter larger than for bulk Si. For larger lattice parameters a strong intensity contrast is found. It is due to the varying Ge/Si concentration which is deduced directly from the intensity ratio at the two energies. Combining the size profile as a function of height from AFM and the lateral size as obtained from the angular scans in ISS yields the evolution of the Ge concentration inside the island as a function of height. The result is illustrated in Fig. 5. The figure clearly shows a rather abrupt interface between pure Si and the SiGe-island, with an almost constant Ge content of roughly 80% above a height of 20 Å. The lattice spacings as a function of the height in the dot (scale on the right) does not follow the sharp Ge concentration change, indicating that the island is highly strained in this region.

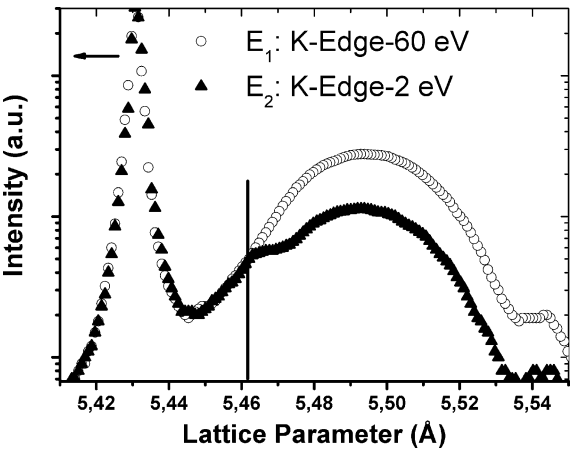

Fig. 4. Anomalous diffraction: intensity close to (800) surface reflection as a function of lattice parameter (from radial scans).

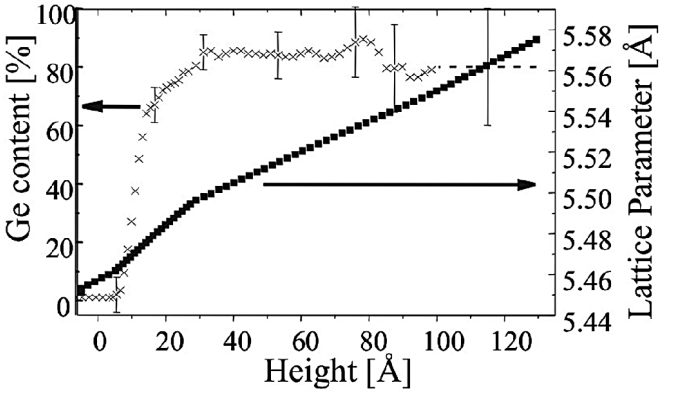

Fig. 5. The lattice parameter (black squares) and the Ge-content (crosses) as a function of the height.

In this example, anomalous diffraction was exploited to determine the average Ge-concentration profile for regions with a common lattice parameter. Malachias et al. extended this method and applied anomalous diffraction also to angular scans [54]. This leads to a particular sensitivity to a gradient of the Ge-concentration in the lateral direction inside the islands. The measurements are performed on a sample grown by chemical vapor deposition of 12 monolayers of pure Ge on Si (001) at 600 °C. The anomalous intensity maps in the q_r, q_a plane close to the (400) surface reflection are shown in Fig. 6(a), (b) for X-ray energies close to the edge and 98 eV below. The extension of the intensity distribution along q_r is, as above, due to the lattice parameter distribution along the growth direction. Since all other experimental details remain unchanged, the detailed analysis of the two maps in the angular direction q_a allows for the determination of the lateral composition in iso lattice parameter slices through the dome. The intensity along q_a for a specific q_r (dashed line in Fig. 6(a), (b)) has been simulated (Fig. 6(c), (d)) by varying the lateral Ge concentration profile. It turns out that the central maximum and the fringes can be fitted for both energies simultaneously by a parabolic profile with a Si rich core and a Ge rich cap layer. Applying the same procedure to all iso strain states, i.e. many q_r positions, it was found that all profiles had a pure Ge border, while the Si concentration in the center varies from 1 at the bottom to 0 at the top of the domes. Combining the lateral size as determined by AFM and the fits to the q_a intensity profile, the height of all iso lattice parameter slices is obtained and hence, a 3D compositional map in real space can be reconstructed, for details see [54].

These results are important tools to further understand the Stranski Krastanow growth of self-assembled coherent islands in strain driven systems, if the strain distribution is known as well. This information is obtained as follows.

3.2. RSM and FEM simulation on $Si_{1-x}Ge_x$/Si(001) islands

$Si_{1-x}Ge_x$/Si(001) islands grown by liquid phase epitaxy (LPE) [56,57] are shaped like truncated pyramids with {111} side facets and a (001) top facet. These samples consist of coherent islands with uniform size and shape. These morphological

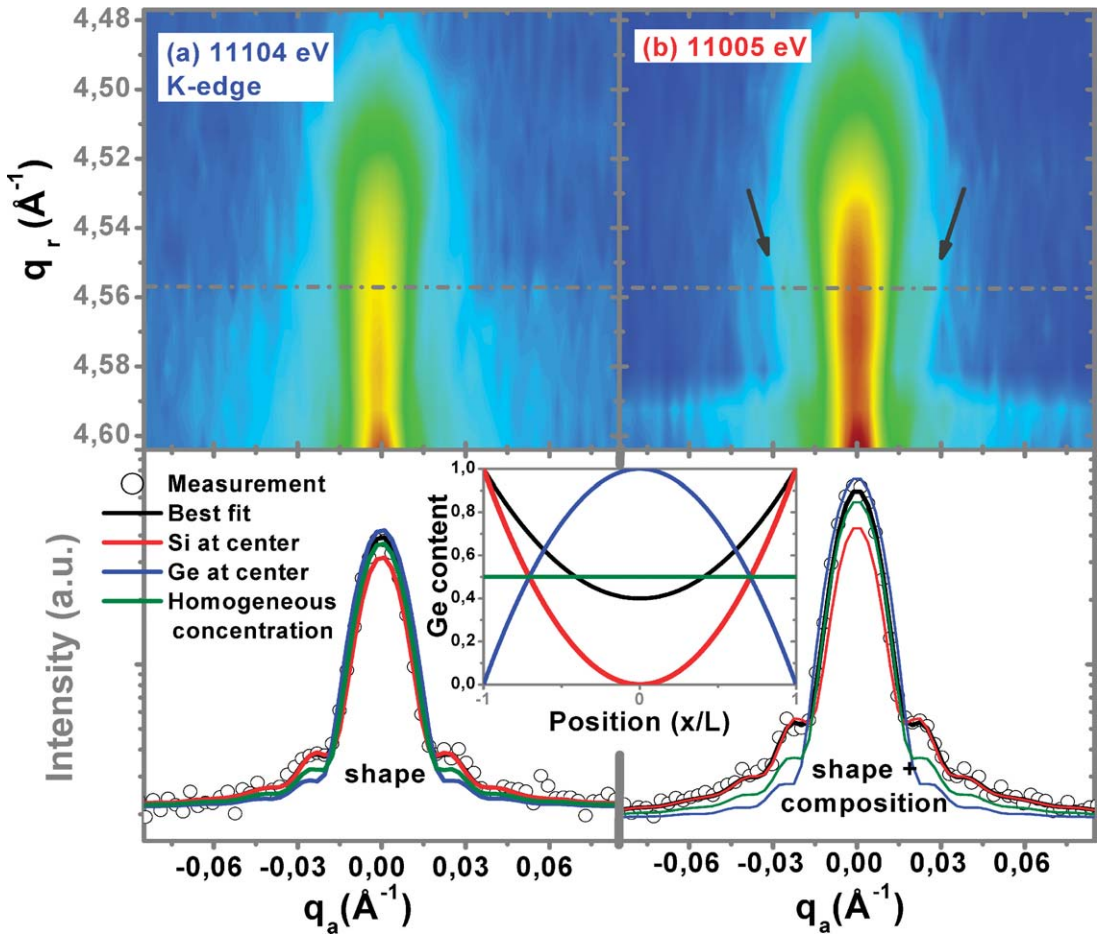

Fig. 6. Anomalous intensity maps in q_r and q_a close to (400) surface reflection from Ge domes at two energies close to the K-edge of Ge. Lower part: angular intensity distribution and simulations with different lateral composition profiles. The profile for the best fir is given in black. For details [54].

parameters are particularly perfect when the growth conditions are chosen close to thermodynamic equilibrium. The specific properties of LPE-grown SiGe islands make them suitable to serve as a model system in the following sense:

- The Stranski–Krastanow growth of three-dimensional islands is still not completely understood. Since LPE is performed rather close to thermodynamic equilibrium, this may clarify the frequently discussed question of to what extent the Stranski–Krastanow growth mode can be discussed in terms of total energy minimization.
- The well-defined size and shape of LPE grown islands allow one to demonstrate the excellent potential of X-ray diffuse scattering for structural characterization.

The detection of a possible chemical composition gradient might serve as a fingerprint of initial stages of growth [58]. The Ge composition can be visualized by X-ray diffuse scattering. Tiny changes in the Ge concentration x inside a SiGe island just lead to a very small effect on the structure amplitude, as given in Eq. (2). Therefore, the main impact on the X-ray diffuse intensity is the strain field that is changing owing to a chemical composition.

Using Eq. (2) and the calculated strain field, the corresponding X-ray diffuse intensity distributions (Fig. 7(a), (b)) is simulated, which can then be compared with the corresponding experimental data shown in Fig. 7(c). Various Ge concentration profiles have been used. Let us first focus on the diffuse scattering from a homogeneous SiGe island, i.e. a constant Ge content of $x = 30\%$ (Fig. 7(a)). A more detailed examination of these calculations shows that the central peak (P1) arises from scattering from the upper half of the island, whereas the butterfly-shaped diffuse intensity P2 around P1 is due to diffuse scattering from sections of the island that are close to the island-substrate interface. One of the most important results is that the upper half of the island is strongly relaxed and exhibits near-cubic symmetry, whereas the lower half of the island is strongly distorted and

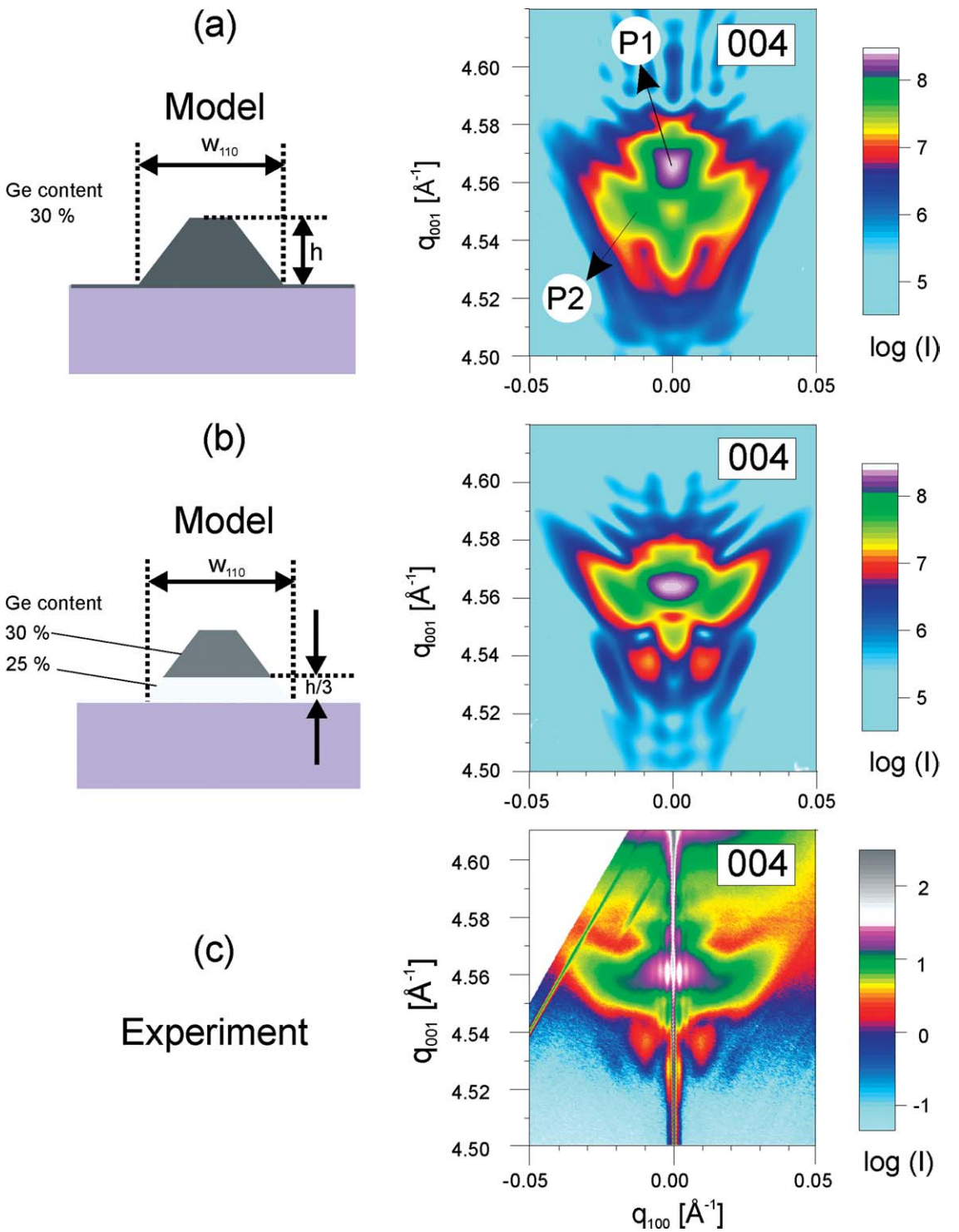

Fig. 7. (a), (b) X-ray diffuse scattering simulations in the vicinity of the 004 reciprocal-lattice point (q_{100}–q_{001}-plane) of an $Si_{1-x}Ge_x$ island with an island base width of $w = 130$ nm and height $h = 65$ nm. The corresponding island models differing in the Ge concentration profile are shown on the left. Scattering from the Si substrate ($q_{001} = 4.628$ Å^{-1}) has been omitted in the simulations. (c) Experiment.

thus gives rise to broad diffuse scattering. The two main features P1 and P2 are accompanied by weak thickness fringes that are due to the finite island height ($h = 65$ nm).

With regard to the results from a homogenous island, the agreement with the experiment can be improved by allowing a variation of the Ge composition inside the island, which is the only free fitting parameter as the island size and shape are well known from SEM and AFM. The simulations clearly prove that the Ge content at the top of the island is significantly higher than in regions at the island base. Surprisingly, an abrupt change of the Ge content at one-third of the island height from $x = 25\%$ to $x = 30\%$ yields the best result (Fig. 7(b)) whereas other simulations using either a linear gradient, a combination of a linear gradient and a constant Ge content or, an abrupt change at one-half of the island height are not satisfactory [39]. Also a simulation using an inclusion with shallow {115} facets clearly fails. The abrupt change of the Ge content can be explained by early stages of growth [58].

4. Conclusion

It has been shown that using a combination of different X-ray scattering techniques the structural parameters of self-assembled nano-structures can be determined with high accuracy and statistical relevance. From grazing incidence small angle scattering size, shape and lateral correlations of uncapped islands are obtained. Grazing incidence *diffraction* adds information on the lattice parameter distribution in the islands, which is shown to be accessible from iso-strain scattering, from which size and strain can be decomposed. In recent years, the near surface sensitivity of grazing incidence techniques, i.e. iso-strain scattering, has been combined with the element specific anomalous dispersion, which allows for an independent analysis of strain and chemical profiles of the elements forming the islands, resulting in a 3D reconstruction of the islands with respect to size, shape, composition and strain. Reciprocal space intensity mapping combined with simulations of the diffuse intensity based on finite element modeling of the displacement field in the islands is a complementary technique. As compared to iso-strain scattering and anomalous grazing incidence diffraction, the advantage is that the elastic response of the substrate is taken into account, while strain and composition in growth direction are evaluated from the diffuse intensity maps close to symmetric or asymmetric reflections. The use of this technique becomes mandatory for buried islands because the monotonic change of the lattice parameter in growth direction breaks down and iso-strain scattering is no longer applicable.

In this article we have focused on demonstrating the merits and limitation of these techniques for the example of free-standing Ge islands on Si (001). The methods have been applied to numerous other important material systems such as InAs on GaAs [25,26,52,59,60], GaN on AlN [61–63], InP on InGaP/GaAs [64], and PbSe on PbEuTe [39,40,65]. In many of these references it is demonstrated that the anomalous version of the scattering methods has considerably improved the techniques and added crucial new information, i.e. on the distribution of strain and composition in these strain driven nano-structures.

X-ray scattering techniques have profited tremendously from the possibilities offered by third generation synchrotron radiation sources. The high brilliance is a prerequisite for high resolution and grazing incidence. The tunability in energy makes the use of contrast enhancement by anomalous dispersion effects feasible. The development of micro beam fabrications is currently underway at many synchrotron radiation sites. It can be foreseen that the resulting small beam cross sections will be utilized to study individual islands in order to quantify the structural parameter variations which are always present in self-organized growth, i.e. far from thermal equilibrium. It will also become possible to exploit the coherence of small beams to directly reconstruct the shape and possibly also the strain in nano-structures as suggested by Vartanyants and Robinson [38].

References

[1] P.M. Petroff, A. Lorke, A. Imamoglou, Epitaxially self-assembled quantum dots, Phys. Today 5 (2001) 46.
[2] Y. Arakawa, H. Sakaki, Multidimensional quantum well laser and temperature dependence of its threshold current, Appl. Phys. Lett. 40 (1982) 939.
[3] F. Klopf, J.P. Reithmayer, A. Forchel, Highly efficient GaInAs/(Al)GaAs quantum-dot lasers based on a single active layer versus 980 nm high-power quantum-well lasers, Appl. Phys. Lett. 77 (2000) 1419.
[4] D. Bimberg, M. Grundmann, N.N. Ledentsov, Quantum Dot Heterostructures, Wiley, New York, 1999.
[5] M. Grundmann, Nano-Optoelectronics, Springer, Berlin, 2002.
[6] V. Shchukin, N.N. Ledentsov, D. Bimberg, Epitaxy of Nanostructures, Springer, Berlin, 2003.
[7] I.N. Stranski, L. Krastanow, Sitzungsber. Akad. Wiss. Wien, Abt. IIb 146 (1937) 797.
[8] D.J. Eaglesham, M. Cerullo, Dislocation-free Stranski–Krastanow growth of Ge on Si(100), Phys. Rev. Lett. 64 (1990) 1943.
[9] Y.-W. Mo, D.E. Savage, B.S. Swartzentruber, M.G. Lagally, Kinetic pathway in Stranski–Krastanov growth of Ge on Si(001), Phys. Rev. Lett. 65 (1990) 1020.
[10] J. Tersoff, F.K. LeGoues, Competing relaxation mechanisms in strained layers, Phys. Rev. Lett. 72 (1994) 3570.
[11] N. Moll, M. Scheffler, E. Pehlke, Influence of surface stress on the equilibrium shape of strained quantum dots, Phys. Rev. B 58 (1998) 4566.

[12] E. Pehlke, N. Moll, A. Kley, M. Scheffler, Shape and stability of quantum dots, Appl. Phys. A 65 (1997) 525.
[13] L.G. Wang, P. Kratzer, N. Moll, M. Scheffler, Size, shape, and stability of InAs quantum dots on the GaAs(001) substrate, Phys. Rev. B 62 (2000) 1897.
[14] L.G. Wang, P. Kratzer, M. Scheffler, N. Moll, Formation and stability of self-assembled coherent islands in highly mismatched heteroepitaxy, Phys. Rev. Lett. 82 (1999) 4042.
[15] Q.K.K. Liu, N. Moll, M. Scheffler, E. Pehlke, Equilibrium shapes and energies of coherent strained InP islands, Phys. Rev. B 60 (1999) 17008.
[16] J. Tersoff, R.M. Tromp, Shape transition in growth of strained islands: spontaneous formation of quantum wires, Phys. Rev. Lett. 70 (1993) 2782.
[17] D.B. Williams, C.B. Carter, Transmission Electron Microscopy – A Textbook for Materials Science, Plenum Press, New York, 1996.
[18] H. Eisele, O. Flebbe, T. Kalka, C. Preinesberger, F. Heinrichsdorff, A. Krost, D. Bimberg, M. Dähne-Prietsch, Cross-sectional scanning-tunneling microscopy of stacked InAs quantum dots, Appl. Phys. Lett. 75 (1999) 106.
[19] J.J. Hren, J.I. Goldstein, Introduction to Analytical Electron Microscopy, Plenum Press, New York, 1979.
[20] L. Reimer, Energy-Filtering Transmission Electron Microscopy, Springer, Berlin, 1995.
[21] R.F. Egerton, Electron Energy-Loss Spectroscopy in the Electron Microscope, Plenum Press, New York, 1996.
[22] R. Schneider, Electron Energy Loss Spectroscopy (EELS), in: Surface and Thin Film Analysis, Wiley-VCH, 2002, p. 50.
[23] R. Schneider, Energy-dispersive X-ray spectroscopy (EDXS), in: Surface and Thin Film Analysis, Wiley-VCH, 2002, p. 194.
[24] G.H. Vineyard, Grazing-incidence diffraction and the distorted-wave approximation for the study of surfaces, Phys. Rev. B 26 (1982) 4146.
[25] I. Kegel, T.H. Metzger, A. Lorke, J. Peisl, J. Stangl, G. Bauer, J.M. Garcia, P.M. Petroff, Nanometer-scale resolution of strain and interdiffusion in self-assembled InAs/GaAs quantum dots, Phys. Rev. Lett. 85 (2000) 1694.
[26] I. Kegel, T.H. Metzger, A. Lorke, J. Peisl, J. Stangl, G. Bauer, K. Nordlund, W.V. Schoenfeld, P.M. Petroff, Determination of strain fields and composition of self-organized quantum dots using X-ray diffraction, Phys. Rev. B 63 (2001) 035318.
[27] M. Schmidbauer, M. Hanke, H. Raidt, R. Köhler, H. Wawra, Strain and composition in SiGe nanoscale islands studied by X-ray scattering, Phys. Rev. B 61 (2000) 5571.
[28] S.K. Sinha, E.B. Sirota, S. Garoff, H.B. Stanley, X-ray and neutron scattering from rough surfaces, Phys. Rev. B 38 (1988) 2297.
[29] T. Salditt, T.H. Metzger, J. Peisl, Kinetic roughness of amorphous multilayers studied by diffuse X-ray scattering, Phys. Rev. Lett. 73 (1994) 2228.
[30] A.J. Steinfort, P.M.L.O. Scholte, A. Ettema, F. Tuinstra, M. Nielsen, E. Landemark, D.-M. Smilgies, R. Feidenhans'l, G. Falkenberg, L. Seehofer, R.L. Johnson, Strain in nanoscale germanium hut clusters on Si(001) studied by X-ray diffraction, Phys. Rev. Lett. 77 (1996) 2009.
[31] G. Springholz, V. Holý, M. Pinczolits, G. Bauer, Self-organized growth of three-dimensional quantum-dot crystals with fcc-like stacking and a tunable lattice constant, Science 282 (1998) 734.
[32] A.A. Darhuber, J. Zhu, V. Holý, J. Stangl, P. Mikulík, K. Brunner, G. Abstreiter, G. Bauer, Highly regular self-organization of step bunches during growth of SiGe on Si(113), Appl. Phys. Lett. 73 (1998) 1535.
[33] M. Rauscher, R. Paniago, H. Metzger, Z. Kovats, J. Domke, J. Peisl, H.-D. Pfannes, J. Schulze, I. Eisele, Grazing incidence small angle X-ray scattering from free-standing nanostructures, J. Appl. Phys. 86 (1999) 6763.
[34] V. Holý, U. Pietsch, T. Baumbach, High Resolution X-Ray Scattering from Thin Films and Multilayers, Springer Tracts Modern Phys., vol. 149, Springer, Berlin, 1999;
U. Pietsch, V. Holý, T. Baumbach, High-Resolution X-Ray Scattering From Thin Films to Lateral Nanostructures, second ed., Advanced Texts in Physics, Springer, Berlin, 2004.
[35] J. Grenzer, N. Darowski, U. Pietsch, A. Daniel, S. Rennon, J.P. Reithmaier, A. Forchel, Grazing-incidence diffraction strain analysis of a laterally-modulated multiquantum well system produced by focused-ion-beam implantation, Appl. Phys. Lett. 77 (2000) 4277.
[36] J. Stangl, A. Daniel, V. Holý, T. Roch, G. Bauer, I. Kegel, T.H. Metzger, Th. Wiebach, Th. Schmidt, O.G. Eberl, Strain and composition distribution in uncapped SiGe islands from X-ray diffraction, Appl. Phys. Lett. 79 (2001) 1474.
[37] R. Lazzari, IsGISAXS: a program for grazing-incidence small-angle X-ray scattering analysis of supported islands, J. Appl. Cryst. 35 (2002) 406.
[38] I.A. Vartanyants, I.K. Robinson, Imaging of quantum array structures with coherent and partially coherent diffraction, J. Synchr. Rad. 10 (2003) 409.
[39] M. Schmidbauer, X-Ray Diffuse Scattering from Self-Organized Mesoscopic Semiconductor Structures, Springer Tracts Modern Phys., vol. 199, Springer, Berlin, 2004.
[40] T.U. Schülli, R.T. Lechner, J. Stangl, G. Springholz, G. Bauer, M. Sztucki, T.H. Metzger, Strain determination in multilayers by complementary anomalous X-ray diffraction, Phys. Rev. B 69 (2004) 195307.
[41] J. Stangl, A. Hesse, T. Roch, V. Holy, G. Bauer, T. Schuelli, T.H. Metzger, Structural investigation of semiconductor nanostructures by X-ray techniques, Nuclear Instrum. Methods Phys. Res. B 200 (2003) 11.
[42] J. Stangl, V. Holy, G. Bauer, Structural properties of self-organized semiconductor nanostructures, Rev. Mod. Phys. 76 (2004) 725.
[43] D. De Salvador, M. Tormen, M. Berti, A.V. Drigo, F. Romanato, F. Boscherini, J. Stangl, S. Zerlauth, G. Bauer, L. Colombo, S. Mobilio, Local lattice distortion in $Si_{1-x-y}Ge_xC_y$ epitaxial layers from X-ray absorption fine structure, Phys. Rev. B 63 (2001) 045314.
[44] I.A. Blech, E. Meieran, Enhanced X-ray diffraction from substrate crystals containing discontinuous surface films, J. Appl. Phys. 38 (1967) 2913.
[45] Q. Shen, S. Kycia, Determination of interfacial strain distribution in quantum-wire structures by synchrotron X-ray scattering, Phys. Rev. B 55 (1997) 15791.

[46] V.M. Kaganer, K.H. Ploog, Energies of strained vicinal surfaces and strained islands, Phys. Rev. B 64 (2001) 205301.
[47] S. Christiansen, M. Albrecht, H.P. Strunk, H.J. Maier, Strained state of Ge(Si) islands on Si: finite element calculations and comparison to convergent beam electron-diffraction measurements, Appl. Phys. Lett. 64 (1994) 3617.
[48] M. Grundmann, O. Stier, D. Bimberg, InAs/GaAs pyramidal quantum dots: strain distribution, optical phonons, and electronic structure, Phys. Rev. B 52 (1995) 11969.
[49] C. Pryor, J. Kim, L.W. Wang, A.J. Williamson, A. Zunger, Comparison of two methods for describing the strain profiles in quantum dots, J. Appl. Phys. 83 (1998) 2548.
[50] F. Buda, J. Kohanoff, M. Parinello, Optical properties of porous silicon: a first-principles study, Phys. Rev. Lett. 69 (1992) 1272.
[51] I. Kegel, T.H. Metzger, J. Peisl, J. Stangl, G. Bauer, D. Smilgies, Vertical alignment of multilayered quantum dots studied by X-ray grazing-incidence diffraction, Phys. Rev. B 60 (1999) 2516.
[52] T. Schülli, M. Sztucki, V. Chamard, T.H. Metzger, D. Schuh, Anomalous X-ray diffraction from InAs/GaAs quantum dot systems, Appl. Phys. Lett. 81 (2002) 448.
[53] T.U. Schülli, J. Stangl, Z. Zhong, R.T. Lechner, M. Sztucki, T.H. Metzger, G. Bauer, Direct determination of strain and composition profiles in SiGe islands by anomalous X-ray diffraction at high momentum transfer, Phys. Rev. Lett. 90 (2003) 066105.
[54] A. Malachias, S. Kycia, G. Medeiros-Ribeiro, R. Magalhaes-Paniago, T.I. Kamins, R. Stanley Williams, 3D composition of epitaxial nanocrystals by anomalous X-ray diffraction: observation of a Si-rich core in Ge domes on Si(100), Phys. Rev. Lett. 91 (2003) 176101.
[55] R. Magalhaes-Paniago, G. Meideros-Ribeiro, A. Malachias, S. Kycia, T.I. Kamins, R. Stanley Williams, Direct evaluation of composition profile, strain relaxation, and elastic energy of Ge:Si(001) self-assembled islands by anomalous X-ray scattering, Phys. Rev. B 66 (2002) 245312.
[56] W. Dorsch, S. Christiansen, M. Albrecht, P.O. Hansson, E. Bauser, H.P. Strunk, Early growth stages of $Ge_{0.85}Si_{0.15}$ on Si(001) from Bi solution, Surf. Sci. 331–333 (1995) 896.
[57] E. Bauser, in: Crystal Growth of Electronic Materials, Elsevier Science, 1985, p. 41.
[58] M. Hanke, M. Schmidbauer, D. Grigoriev, H. Raidt, P. Schäfer, R. Köhler, A.-K. Gerlitzke, H. Wawra, SiGe/Si(001) Stranski–Krastanow islands by liquid-phase epitaxy: diffuse X-ray scattering versus growth observations, Phys. Rev. B 69 (2004) 075317.
[59] I. Kegel, T.H. Metzger, P. Fratzl, J. Peisl, A. Lorke, J.M. Garcia, P.M. Petroff, Interdependence of strain and shape in self-assembled coherent InAs islands on GaAs, Europhys. Lett. 45 (1999) 222.
[60] S. Grenier, M.G. Proietti, J.M. Garcia, J. Garcia, Grazing-incidence diffraction anomalous fine structure of InAs/InP(001) self-assembled quantum wires, Europhys. Lett. 57 (4) (2002) 499.
[61] V. Chamard, T.H. Metzger, E. Bellet-Amalric, B. Daudin, C. Adelmann, H. Mariette, G. Mula, Structure and ordering of GaN quantum dot multilayers, Appl. Phys. Lett. 79 (2001) 1971.
[62] V. Chamard, T.H. Metzger, M. Sztucki, V. Holý, M. Tolan, E. Bellet-Amalric, C. Adelmann, B. Daudin, H. Mariette, On the driving forces for the vertical alignment in nitride quantum dot multilayers, Europhys. Lett. 63 (2003) 268.
[63] V. Chamard, T. Schülli, M. Sztucki, T.H. Metzger, E. Sarigiannidou, J.-L. Rouviere, M. Tolan, C. Adelmann, B. Daudin, Strain distribution in nitride quantum dot multilayers, Phys. Rev. B 69 (2004) 125327.
[64] M. Schmidbauer, F. Hatami, M. Hanke, P. Schäfer, K. Braune, W.T. Masselink, R. Köhler, M. Ramsteiner, Shape-mediated anisotropic strain in self-assembled $InP/In_{0.48}Ga_{0.52}P$ quantum dots, Phys. Rev. B 65 (2002) 125320.
[65] R.T. Lechner, T.U. Schülli, V. Holý, G. Springholz, J. Stangl, A. Raab, G. Bauer, T.H. Metzger, Ordering parameters of self-organized three-dimensional quantum-dot lattices determined from anomalous X-ray, Appl. Phys. Lett. 84 (2004) 885.